Construction C/g-C$_3$N$_4$ with synergistic performance toward high photocatalytic performance

Qingbo Yu*, Huiqin Li, Kuan Yang and Qixiang Xu

Department of Materials Science and Engineering,
Anhui University of Science and Technology,
Huainan, 232001, China
Email: yuqingbo007@163.com
Email: 1145667468@qq.com
Email: 826245354@qq.com
Email: 2697001010@qq.com
*Corresponding author

Xianhua Li

School of Artificial Intelligence,
Anhui University of Science and Technology,
Huainan, 232001, China
Email: 4774896@qq.com

Abstract: Aromatic carbon (C) doped graphitic carbon nitride (g-C$_3$N$_4$) is one of the effective strategies to improve the photocatalytic performance of g-C$_3$N$_4$. The present work developed a feasible method to construct C/g-C3N4 through carbonising the mixture of g-C3N4 and phenol-formaldehyde (PF) obtained in situ polymerisation. This synthesis method not only improves the interaction between PF and g-C$_3$N$_4$, but also promotes the preparation of aromatic carbon-doped g-C$_3$N$_4$ in the subsequent calcinations process. The resulted C/g-C$_3$N$_4$-600 catalysts show developed optoelectronic properties, superior photocatalytic activity and higher surface area (1336 cm^2 g^{-1}) due to the extended π-conjugation system and distinctive morphology.

Keywords: C/g-C3N4; optoelectronic properties; surface area; photocatalytic properties; phenol-formaldehyde; polymerisation; surface area; conjugation; morphology.

Biographical notes: Qingbo Yu is a Professor in Anhui University of Science and Technology. He completed her doctoral work at Anhui University. Her research interests are in polymer materials and nanocomposites.

Huiqin Li is a postgraduate student in Anhui university of Science and Technology. Her research interests include nanomaterials, porous materials, biosensors.

Kuan Yang is a postgraduate student in Anhui university of Science and Technology. He mainly engaged in the preparation of materials and the research of photocatalytic degradation.

Qixiang Xu is a postgraduate student in Anhui university of Science and Technology. He mainly engaged in the research of photocatalytic degradation.

Xianhua Li is a Professor in Anhui University of Science and Technology. He completed her doctoral work at Shanghai University. His research interests are in functional materials.

1   Introduction

Polymeric graphitic carbon nitride (g-C_3N_4) has drawn tremendous attention in photocatalytic degradation because of its very large excitation binding energy, nontoxicity and highly physicochemical stability (Liu and Cohen, 1989; Zhang et al., 2013; Zhu et al., 2014). However, g-C_3N_4 suffers from the rapid recombination of electron-hole pairs, low visible light absorption, and poor surface are a caused by the strong van der Waals attractions between sp^2 carbon atoms (Gillan, 2000).

To improve these short comings of g-C_3N_4, previous reports have employed strategies such as nanostructure engineering, electronic structure modulation, and coupling with other function materials (Su et al., 2013; Yu et al., 2014; Zeng et al., 2016; Guo et al., 2017; Ma et al., 2017). Apart from above-mentioned methods, carbon-doped g-C_3N_4-based composite photocatalysts can enhance the superior combination property, such as suppressing the recombination of photogenerated charges, and easy to recycle. Panneri et al. (2017) demonstrated the efficient removal of tetracycline antibiotic by carbon-doped g-C_3N_4. Chuang et al. (2016) extended the π-conjugation of g-C_3N_4 by incorporating aromatic carbon, resulting in enhanced photocatalytic H_2 evolution. Yet most studies only consider one aspect of disadvantages, and ignore the other aspects. Therefore, there is still an urgent call for a novel and effective method to interconnect various aspects of performance.

In this work, a mixture of g-C_3N_4 and phenol-formaldehyde (PF) obtained by in-situ polymerisation was calcined to prepare the C/g-C_3N_4 photocatalyst with photo-induced carrier separation, high visible light absorption, and improved specific surface area. From Figure 1, the phenol and formaldehyde are the raw materials of carbon. Firstly, the formaldehyde-solvated g-C_3N_4 was obtained by hydrogen bonds between the two. Then, the polymerisation occurred in a Teflon-lined autoclave after adding phenol and $ZnCl_2$. The PF in the obtained sample prevented the agglomeration of g-C_3N_4. Finally, the PF/g-C_3N_4 mixture was heated under a flowing nitrogen atmosphere to form the C/g-C_3N_4 photocatalyst. There are two processes in carbonisation process. First, the g-C_3N_4 may incorporate with C in aromatic heterocycles by annealing, because of the π-π interaction between PF and g-C_3N_4.

Figure 1 The process of the C/g-C₃N₄ photocatalyst (see online version for colours)
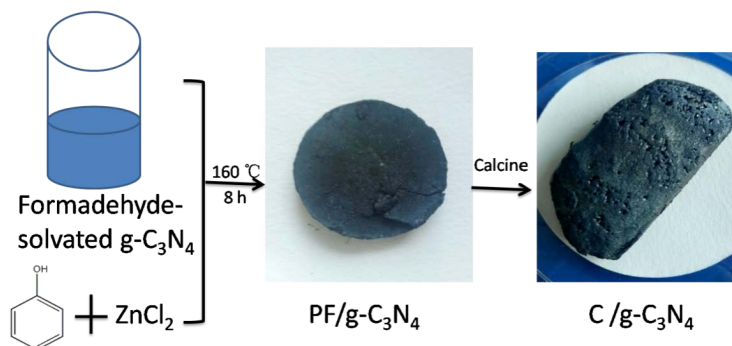
This may extend the delocalisation of electrons in the π-conjugation system, promoting charge separation and transportation (Zhou et al., 2016). Second, the C produced from PF annealing using ZnCl₂ as foaming agent and porogen (Yu et al., 2016), which can improve the adsorption capacity of photocatalysts. Thus, the obtained photocatalysts may exhibit high photocatalytic activity due to bifunctional effects caused by C and highly dispersed g-C₃N₄ in C-based, such as extended π-conjugation, large specific surface area, high transmission of photogenerated charges.

2   Experimental

2.1   Synthesis of C/g-C₃N₄ catalysts

The g-C₃N₄ was prepared using our previous method (Yu et al., 2014). For C/g-C₃N₄preparation, we mixed formaldehyde (1.5 mL) and g-C₃N₄ (0.3 g) by ultrasonic, obtaining solvated g-C₃N₄ by hydrogen bonds. Then, the phenol (0.491 g) and zinc chloride (6 g, ZnCl₂) were added. The viscous sol was transferred to a sealed autoclave, followed by heating at 160°C for 8 h. The obtained mixture was dried and carbonised in the atmosphere of nitrogen. The C/g-C₃N₄ was purified in 1M HCl several times, and then filtered and dried. The obtained sample was signed as C/g-C₃N₄-550, C/g-C₃N₄-600 and C/g-C₃N₄-800 according the carbonisation temperature changed from 550°C, 600°C to 800°C. In order to understand the role of carbon, it has been preparing through calcination the phenol-formalhehude (PF) obtained in suit polymerisation, which is similar to the above mentioned. The carbon was signed as C-550, C-600 and C-800 according the carbonisation temperature (550°C, 600°C and 800°C). In addition, we have calcined g-C₃N₄ again at 600°C for 1.5 h. The sample was signed as g-C₃N₄-1.

2.2   Characterisation

A UV–vis spectrophotometer was conducted using Varian CARY 100, USA. The morphology of the samples was inspected using field-emission scanning electron microscopy (SEM). The structure of the samples was determined according to X-ray diffraction (XRD Rigaku RINT2000 diffractometer), X-ray photoelectron spectra (XPS Thermo ESCALAB 250) and Fourier transform spectrophotometer (FTIR). The Q2000 thermogravimetric analyser was measured using thermo gravimetric analysis (TGA) in

argon gas. The electrochemical measurements were reported by the CHI 660E electrochemical workstation using three electrode cells.

2.3   *The photocatalytic activity*

Using Methylene blue (MB) as a model, the photocatalytic ability of the samples were carried out under visible light irradiation (>420 nm). In detail, the obtained catalysts (3 mg) were put in MB (62 μM) aqueous solution. After saturated adsorption, the degradation of MB solution was   by UV-vis spectrophotometer (664 nm).

3   **Results and discussion**

As shown by the TGA curves in Figure 2(a), the PF, g-C_3N_4 and PF/g-C_3N_4 have similar weight loss pattern. However, the PF/g-C_3N_4fabricated by polymerisation PF precursor in presence of g-C_3N_4 (Figure 2(a)-1), shows a slow weight loss comparing with original g-C_3N_4 and PF (Figure 2(a)-2 and 2(a)-3), implying thermally more stable. The decomposition of PF/g-C_3N_4, shown in DTA curve, occurs at higher temperature compared with PF (Figure 2(b)). The reason may be the interaction between PF and g-C_3N_4 when the polymerisation is performed using phenol (P) and formaldehyde as precursor of PF. This can be confirmed by FTIR spectra. From Figure 3(a)-2, the band at 1606 cm^{-1} equivalent of stretching vibration mode of the conjugated structure in PF. The breathing mode of C=N in g-C_3N_4 is characterised by the band at 1637 cm^{-1} (Figure 3(a)-3). Nevertheless, for PF/g-C_3N_4, it moves to 1633 cm^{-1} (Figure 3(a)-1). In addition, the colour of the sample also changed after the polymerisation of PF precursor in the presence of g-C_3N_4. The colour of PF is red-brown (Figure 3(c)). The g-C_3N_4 is yellow (Figure 3(b)). However, the colour of the PF/g-C_3N_4 is black (Figure 1). All of these indicate that there is interaction between PF and g-C_3N_4, which improve the stability of PF/g-C_3N_4.

Figure 2   TGA (a) and DTG (b) curves of the PF/g-C_3N_4 (1), g-C_3N_4 (2) and PF (3)
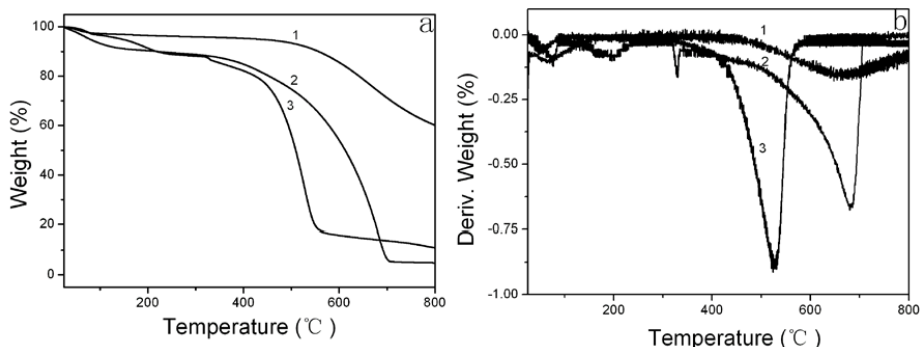
It is well known that carbon can enhance the electrical conductivity and impede the electron hole recombinations (Panneri et al., 2017). In this paper, the interaction between PF and g-C_3N_4 may be able to improve the effect of C. So the C/g-C_3N_4 using PF as a C source was prepared by changing carbonisation temperature.

Figure 3   FTIR spectra (a) of (1) PF/g-C$_3$N$_4$, (2) PF and (3) g-C$_3$N$_4$; photos of g-C$_3$N$_4$ (b) and PF (c) (see online version for colours)
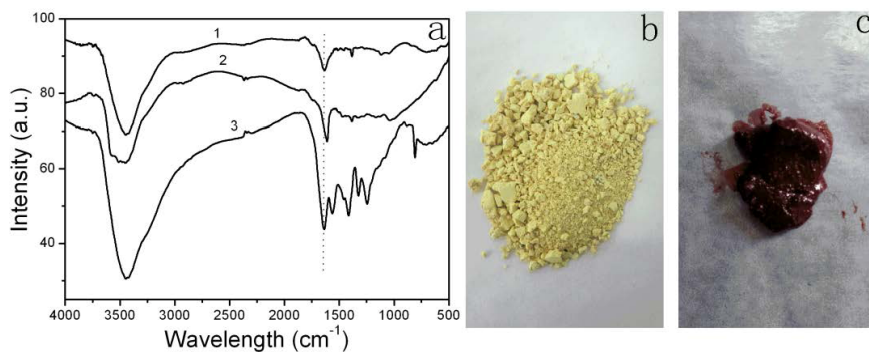
FTIR spectra are displayed in Figure 4. Compared with the C (Figure 4(a)-1), all the C/g-C$_3$N$_4$ preparation temperature from 550°C to 800°C (Figure 4(a)-2, 4(a)-3, and 4(a)-4) showed an additional peak at 1563 cm^{-1}, which equivalent of the stretching of C-N in g-C$_3$N$_4$ (Figure 4(a)-5). The band at 1637 cm^{-1} for g-C$_3$N$_4$ (Figure 4(a)-5) is attributed to C=N stretching (Bousetta et al., 1994). To carbon, the band at 1620 cm^{-1} is attributed to the breathing mode of C=C (Figure 4(a)-1). However, the broad band at 1637-1620 cm^{-1} is shown in C/g-C$_3$N$_4$. This FTIR analysis confirmed not only the existence of g-C$_3$N$_4$ in C/g-C$_3$N$_4$, but also an interaction between C and g-C$_3$N$_4$ thanks to the preparation process.

Figure 4   FTIR (a) and XRD (b) spectra of (1) C-550, (2) C/g-C$_3$N$_4$-550, (3) C/g-C$_3$N$_4$-600, (4) C/g-C$_3$N$_4$-800 and (5) g-C$_3$N$_4$ (inset is the XRD spectra)
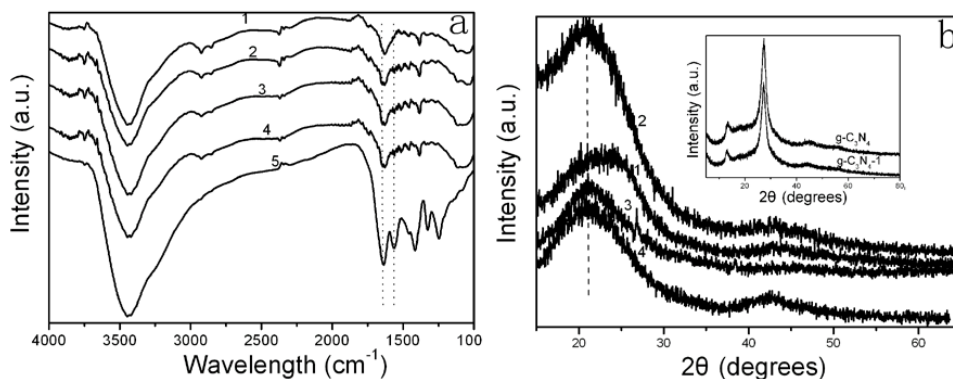
XRD analysis of samples are displayed in Figure 4(b). The C/g-C$_3$N$_4$ preparation temperature from 550°C to 800°C have similar XRD curve with C. The difference is that the XRD peak of C/g-C$_3$N$_4$ exhibit a broad peak at around 21.3° and the C shows at around 23.3°. The reason may be that the inaction between C and g-C$_3$N$_4$ confirmed by FTIR. However, there is not the XRD peak of g-C$_3$N$_4$ (inset in Figure 4(b)). In fact, the calcining of g-C$_3$N$_4$ do not change the stacking structure, there are similar XRD curve for the g-C$_3$N$_4$ and g-C$_3$N$_4$-1 (inset in Figure 4(b)). So the missing of XRD peak at 27.4° in C/g-C$_3$N$_4$ may be that the content of g-C$_3$N$_4$ is too small to be shown.

Figure 5 displays the XPS analysis of g-C_3N_4 and C/g-C_3N_4. From C 1s spectra in Figure 5(a) and (c), the peak at 284.7 eV, 285.2 eV, 286.4 eV and 288.5 eV are utilised to graphitic C=C, C-NH_2 species and SP^2-hybridised carbon, respectively. The high-resolution N 1s spectra are shown in Figure 5(b) and (d). Two peaks are observed at 399.4 eV and 400.9 eV, corresponding to N atoms in N-$(C)_3$ and the end of amino groups, respectively (Ma et al., 2017). By contrast in C 1s spectra (Figure 5(c) and (a)), the peaks intensity of 284.7 eV and 285.2 eV are increased in Figure 5(c). While the peak at 397.7 eV in N 1s spectra (Figure 5(d)) is decreased comparing with Figure 5(b). Furthermore, the C/N ratio of C/g-C_3N_4 implied an increase from 1.4 for g-C_3N_4 to 45.9 estimated from the XPS analysis. The results imply that the deficiency of N in C/g-C_3N_4 prompted by calcinations process, and subsequent in situ doping of carbon from the residue of phenol-formaldehyde resin (PF) burned out (Panneri et al., 2017). This may provide novel optoelectronic properties.

Figure 5   XPS patterns (a) C 1s and (b) N 1s of g-C_3N_4 and (c) C 1s and (d) N 1s of C/g-C_3N_4
(see online version for colours)
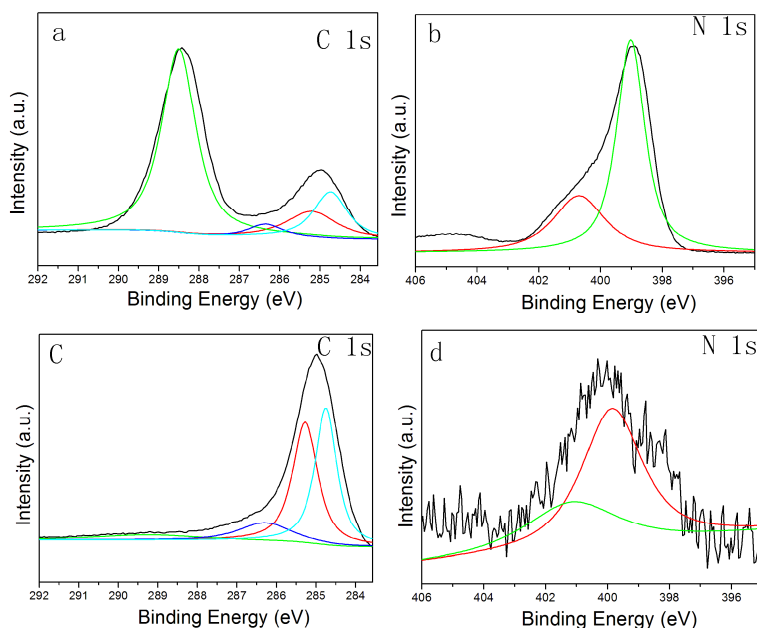
The light absorption of the samples was investigated by UV-vis spectra. From Figure 6(a), the C/g-C_3N_4 preparation temperature from 550°C to 800°C have similar curve with C, which possess broad light absorption intensity in the whole regions comparing with g-C_3N_4. This is a typical behaviour of carbon-based materials, attributing to narrower gap of the sp2 carbon cluster embedded in C (Pan et al., 2010).

To investigate photocurrent responses of C/g-C_3N_4 with different preparation temperature, i-t curves were measured displayed in Figure 6(b). It can be seen that photocurrent responses via on-off cycles were observed in these samples, implying separation efficiency of photogenerated carriers under visible-light irradiation. The photocurrent enhancement of C/g-C_3N_4 is higher than that of pristine g-C_3N_4, indicating an enhanced photoinduced separation of electron/hole pairs. This can be attributed to the

formation of the interaction between C and g-C$_3$N$_4$, which enhances large delocalised π bonds, promotes electrical conductivity and impedes the electron hole recombinations.

Figure 6   UV-vis spectra (a) and periodic on/off photocurrent of (1) C-550, (2) C/g-C$_3$N$_4$-550, (3) C/g-C$_3$N$_4$-600, (4) C/g-C$_3$N$_4$-800 and (5) g-C$_3$N$_4$
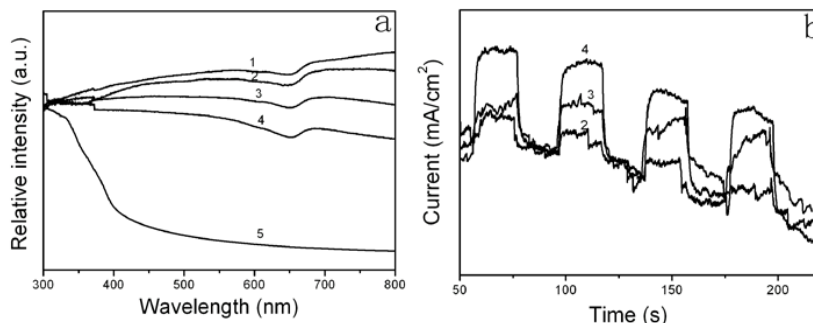
The adsorption capability of the catalyst is important. It can not only make the catalyst behave as a collector to gather the dye without sunlight, but also enhance photodetradation reactions owing to efficient dye-photosensitisation. From Figure 7(a), the adsorption capability of g-C$_3$N$_4$ is about 60 mol/g. No matter how the calcination temperature the C/g-C$_3$N$_4$ nanocomposites had been, its adsorption capacity is high. This can be attributed to the high adsorption capacities of C with corresponding calcination temperature. However, it is worth noting that the adsorption capacity of C/g-C$_3$N$_4$-600 is higher than that of g-C$_3$N$_4$ and C-600. This can be explained using SEM and BET analysis.

Figure 7   Adsorption capacity (a) and N$_2$ adsorption−desorption isotherms (b, c and d) of samples
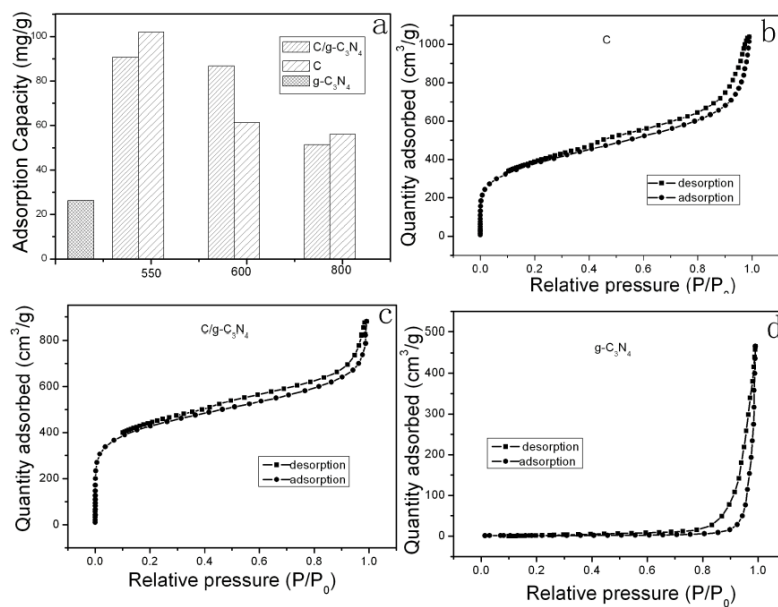
The nitrogen adsorption-desorption isotherems are exhibited in Figure 7. The surface area of C is 1190 $cm^2 g^{-1}$ (Figure 7(b)). However, the C/g-C_3N_4 shows a relatively high surface area (1336 $cm^2 g^{-1}$, Figure 7(c)), which is much higher than that of g-C_3N_4 (4.7 $cm^2 g^{-1}$, Figure 7(d)). The reason may be contributed to the hollow structure. The result indicates that the C/g-C_3N_4 will possess higher photocatalytic degradation.

Figure 8 shows the SEM of C and C/g-C_3N_4 with different carbonisation temperatures. With the increase of carboniation temperatures, the micrograph of C changed significantly and the appearance became more uniform (Figure 8(a)–(c)). The trend for C/g-C_3N_4 is similar to that of C (Figure 8(d)–(f)). However, the magnified SEM image can observe clearly that the composite structure assembled ball and rod becomes a finer fibrous structure (Figure 8(g)–(i)). It is worth noting that the morphology of the C/g-C_3N_4-600 is special. Compared to Figure 8(g) and (i), the rod is hollow (Figure 8(h)), which may increase the specific surface area, thus improving the adsorption capacity.

Figure 8   FESEM images of: (a) C-550; (b) C-600; (C) C-800; (d) and (g) C/g-C_3N_4-550; (e) and (h) C/g-C_3N_4-600 and (f) and (i) C/g-C_3N_4-800
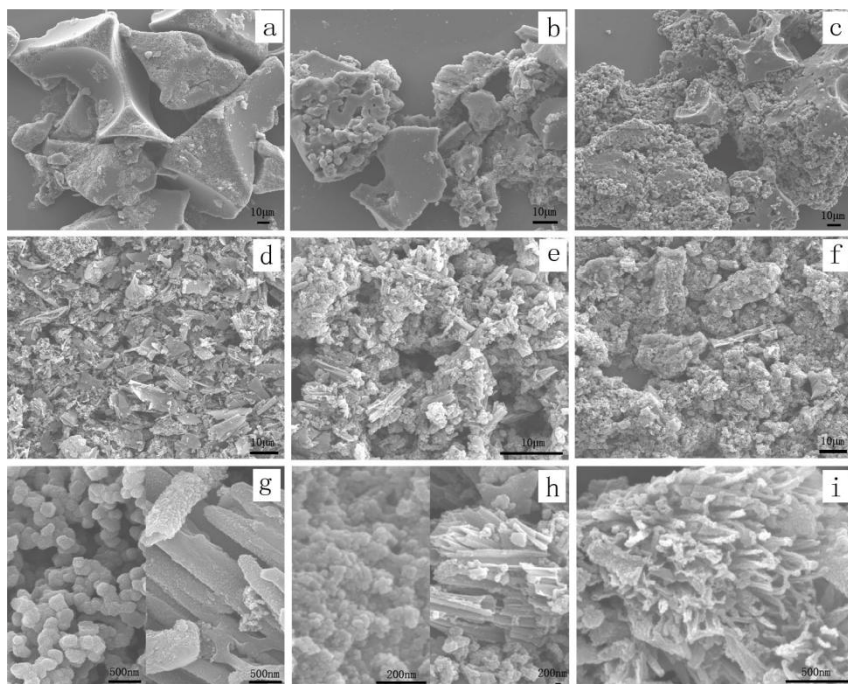
The photocatalytic experiments using MB as a model pollutant are shown in Figure 9. The C/g-C_3N_4-600 shows the highest photocatalytic performance in the as-synthesised samples, which is attributed to the higher surface area, improved interaction between C and g-C_3N_4 and superior optoelectronic properties. However, the photocatalytic performance decreases when the carbonisation temperature is changed. Especially, the C/g-C_3N_4-550 shows lower photocatalytic degradation compared to the pristine g-C_3N_4. The reason may be attributed to the different morphology, which caused the changing surface area.

Figure 9 Photocatalytic degradation of sample
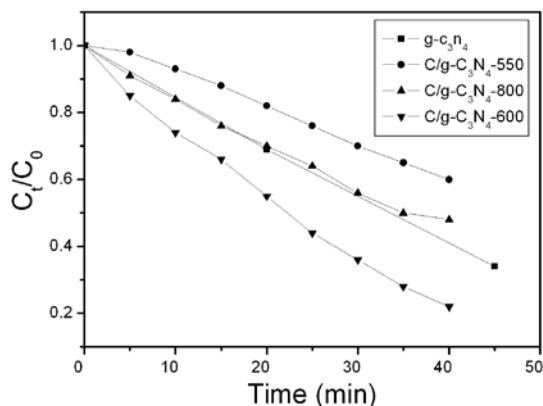
4 Conclusion

For this study, we developed a feasible route to prepare C/g-C$_3$N$_4$-600, which possess enhanced light absorption owing to the C, improved adsorption capacity due to higher surface area, and suppressed recombination of photogenerated charges owing to the interaction between C and g-C$_3$N$_4$. The process for the preparation of the mixture of PF and g-C$_3$N$_4$ plays the key role. The interaction between PF and g-C$_3$N$_4$ by in situ polymerisation enhances the carbon doped g-C$_3$N$_4$ in the subsequent calcination process. The use of the devised method facilitated charge separation, higher surface area, available material contact and high photocatalytic degradation.

Acknowledgments

References

Bousetta, A., Lu, M. and Bensaoula, A. (1994) 'Formation of carbon nitride films on Si (100) substrates by electron cyclotron resonance plasma assisted vapor deposition', *Appl. Phys. Lett.*, Vol. 65, pp.696–698.

Chuang, P., Wu, K., Yeh, T. and Teng, H. (2016) 'Extending the πConjugation of g-C$_3$N$_4$ by incorporating aromatic carbon for photocatalytic H$_2$ evolution from aqueous solution', *ACS Sustainable Chem. Eng.*, Vol. 4, pp.5989−5997.

Gillan, E.G. (2000) 'Synthesis of nitrogen-rich carbon nitride networks from an energetic molecular azide precursor', *Chem. Mater.*, Vol. 12, pp.3906−3912.

Guo, F., Shi, W., Guan, W., Huang, H. and Liu, Y. (2017) 'Carbon dots/g-C$_3$N$_4$/ZnO nanocomposite as efficient visible-light driven photocatalyst for tetracycline total degradation', *September Purif. Technol.*, Vol. 173, pp.295–303.

Liu, A.Y. and Cohen, M.L. (1989) 'Prediction of new low compressibility solids', *Science*, Vol. 245, pp.841−842.

Ma, L., Fan, H., Fu, K., Lei, S., Hu, Q. and Huang, H. (2017) 'Protonation of graphitic carbon nitride (g-C_3N_4) for an electrostatically self-assembling carbon@g-C_3N_4 core−Shell nanostructure toward high hydrogen evolution', *ACS Sustainable Chem. Eng.*, Vol. 5, pp.7093−7103.

Pan, D., Zhang, J., Li, Z., Wu, C., Yan, X. and Wu, M. (2010) 'Observation of pH-, solvent-, spin-, and excitation-dependent blue photoluminescence from carbon nanoparticles', *Chem. Commun.*, Vol. 21, pp.3681–3683.

Panneri, S., Ganguly, P., Mohan, M., Nair, B., Mohamed, A., Warrier, K. and Hareesh, U. (2017) 'Photoregenerable, bifunctional granules of carbon-doped g-C_3N_4 as adsorptive photocatalyst for the efficient removal of tetracycline antibiotic', *ACS Sustainable Chem. Eng.*, Vol. 5, pp.1610−1618.

Su, F.L., Lu, J.W., Tian, Y., Ma, X.B. and Gong, J.L. (2013) 'TiO_2 nanoarrays sensitized with CdS quantum dots for highly efficient photoelectrochemical water splitting', *Phys. Chem. Chem. Phys.*, Vol. 15, pp.12026−12032.

Yu, Q., Guo, S., Li, X. and Zhang, M. (2014) 'Template free fabrication of porous g-C_3N_4/graphene hybrid with enhanced photocatalytic capability under visible light', *Mater. Technol*, Vol. 3, pp.172–178.

Yu, Q., Li, X., Zhang, M. (2014) 'One-step fabrication and high photocatalytic activity of porous graphitic carbon nitride synthesised via direct polymerisation of dicyandiamide without templates', *Micro Nano Lett.*, Vol. 1, pp.1–5.

Yu, Z., Li, G., Fechler, N., Yang, N., Ma, Z., Wang, X., Antonietti, M. and Yu, S. (2016) 'Polymerization under hypersaline conditions: a robust route to phenolic Polymer-derived carbon aerogels', *Angew. Chem. Int. Ed.*, Vol. 55, pp.14623–14627.

Zeng, Y.P., Wang, Y., Chen, J.W., Jiang, Y.W., Kiani, M., Li, B.Q. and Wang, R.L. (2016) 'Fabrication of high-activity hybrid niTiO_3/g-C_3N_4 Heterostructured photocatalysts for water splitting to enhanced hydrogen production', *Ceram. Int.*, Vol. 42, 12297−12305.

Zhang, Y., Pan, Q., Chai, G., Liang, M., Dong, G., Zhang, Q. and Qiu, J. (2013) 'Synthesis and luminescence mechanism of multicolor-emitting g-C_3N_4 nanopowders by low temperature thermal condensation of melamine', *Sci. Rep.*, Vol. 3, pp.1–8.

Zhou, Y., Zhang, L., Huang, W., Kong, Q., Fan, X., Wang, M. and Shi, J. (2016) 'N-doped graphitic carbon-incorporated g-C_3N_4 for remarkably enhanced photocatalytic H_2 evolution under visible light', *Carbon*, Vol. 99, pp.111−117.

Zhu, J., Xiao, P., Li, H. and Carabineriro, S. (2014) 'Graphitic carbon nitride: synthesis, properties, and applications in catalysis', *ACS Appl. Mater. Interfaces*, Vol. 6, pp.16449−16465.